

A fermionic portal to a non-abelian dark sector

Alexander Belyaev,^{1,*} Aldo Deandrea,^{2,†} Stefano Moretti,^{1,3,‡} Luca Panizzi,^{1,3,§} and Nakorn Thongyoi^{1,¶}

¹*School of Physics and Astronomy, University of Southampton, Highfield, Southampton SO17 1BJ, UK*

²*Univ. Lyon, Université Claude Bernard Lyon 1,*

CNRS/IN2P3, IP2I UMR5822, F-69622, Villeurbanne, France

³*Department of Physics and Astronomy, Uppsala University, Box 516, SE-751 20 Uppsala, Sweden*

We introduce a new class of renormalisable models, consisting of a dark $SU(2)_D$ gauge sector connected to the Standard Model (SM) through a Vector-Like (VL) fermion mediator, not requiring a Higgs portal, in which a massive vector boson is the Dark Matter (DM) candidate. These models are labelled Fermion Portal Vector Dark Matter (FPVDM). Multiple realisations are possible, depending on the properties of the VL partner and of the scalar potential. One example is discussed in detail. FPVDM models have a large number of applications in collider and non-collider experiments, depending on the mediator sector.

The nature of DM, which existence has been established beyond any reasonable doubt by several independent cosmological observations, is one of the greatest puzzles of contemporary particle physics. Models with a vector DM, especially in the non-abelian case, are the least explored but well motivated, as the gauge principle offers guidance and constraints limiting the possible theoretical constructions (see, e.g., [1–16] for a discussion of non-abelian DM in different set-ups, in particular using non-renormalisable kinetic mixing terms or Higgs portal scenarios). In this letter we suggest a new framework which extends the gauge sector of the Standard Model (SM) by a new non-abelian gauge group for which no renormalisable kinetic mixing terms are allowed¹ and under which all SM particle are singlets. The simplest non-abelian group is $SU(2)$, which in the following will be labelled $SU(2)_D$ as it connects the SM to the dark sector. The gauge bosons associated to $SU(2)_D$ are labelled as $V_\mu^D = (V_{D+\mu}^0 \ V_{D0\mu}^0 \ V_{D-\mu}^0)$, where, here and in the following, the electric charge is specified in the fields superscripts, while the isospin under $SU(2)_D$ (D-isospin) is specified in the fields subscripts. The covariant derivative associated with $SU(2)_D$ is:

$$D_\mu = \partial_\mu - \left(i \frac{g_D}{\sqrt{2}} V_{D\pm\mu}^0 T_D^\pm + i g_D V_{D0\mu}^0 T_{3D} \right), \quad (1)$$

where g_D is the $SU(2)_D$ coupling constant and T_{3D} is the D-isospin.

The fields responsible for breaking the gauge symmetries are two scalar doublets:

$$\begin{aligned} \Phi_H &= (\phi^+ \ \phi^0)^T \rightsquigarrow \langle \Phi_H \rangle = \frac{1}{\sqrt{2}} (0 \ v)^T, \\ \Phi_D &= \left(\varphi_{D+\frac{1}{2}}^0 \ \varphi_{D-\frac{1}{2}}^0 \right)^T \rightsquigarrow \langle \Phi_D \rangle = \frac{1}{\sqrt{2}} (0 \ v_D)^T, \end{aligned} \quad (2)$$

where the first is breaking $SU(2)_L \times U(1)_Y$, while the second is breaking $SU(2)_D$ via their respective Vacuum Expectation Values (VEVs) v and v_D .

A \mathbb{Z}_2 symmetry is then introduced to stabilise the DM candidate associated with the lightest \mathbb{Z}_2 -odd particle of the model. It is assumed that different members of the same $SU(2)_D$ multiplet have a different \mathbb{Z}_2 parity, while all SM states are even under \mathbb{Z}_2 . The fact that SM fields are neutral under the D-charge has a remarkable consequence: the lightest D-charged and electrically-neutral state is stable and is therefore a dark matter candidate.

The possible origin of the \mathbb{Z}_2 parity can be, for example, linked to an additional $U(1)_D$ which would also introduce a kinetic mixing between $U(1)_Y$ and $U(1)_D$. Another possibility is the underlying strongly-coupled sector which condensates form particles in the low energy regime. A detailed discussion of this case is given in [18] and further used in [19] for a scalar DM candidate.

A DM candidate which is charged under a new dark gauge group can potentially induce a phase of dark matter genesis in the early universe, as discussed in the $U(1)_D$ case in [17], which can be used to explain the tension in the measurement of the Hubble constant from Planck and supernovae data. We do not explore this interesting possibility as it requires a dedicated study and goes beyond the minimal model set-up we wish to discuss here.

The connection between the SM and the dark sector is provided by two new VL fermions, which are singlets of $SU(2)_L$ but form a doublet under $SU(2)_D$, $\Psi = (\psi_D \ \psi)^T$.² This fermion doublet contains a \mathbb{Z}_2 -odd component and a \mathbb{Z}_2 -even component, which without loss of generality can be identified with the $T_{3D} = +1/2$ and $T_{3D} = -1/2$ D-isospin components, respectively: the latter can mix with SM fermions which share the same SM quantum numbers. The mass and interaction Lagrangian of the fermion sector is:

$$-\mathcal{L}_f = M_\Psi \bar{\Psi} \Psi + (y \bar{f}_L^{\text{SM}} \Phi_H f_R^{\text{SM}} + y' \bar{\Psi}_L \Phi_D f_R^{\text{SM}} + h.c.), \quad (3)$$

¹ Contributions to gauge kinetic mixing may arise at loop level, depending on the structure of the Higgs sector, but they correspond to suppressed higher operator terms.

² VL portals have also been explored in [20, 21], but for scalar DM candidates.

where $f_{L,R}^{\text{SM}}$ generically denotes a SM left-handed doublet or right-handed singlet, y is the Yukawa coupling of the SM and y' is a new Yukawa coupling connecting the SM fermion with Ψ . The particle content of the model, which we abbreviate as FPVDM, is summarised in tab. I.

	$SU(2)_L$	$U(1)_Y$	$SU(2)_D$	\mathbb{Z}_2
$\Phi_D = \begin{pmatrix} \varphi_{D+\frac{1}{2}}^0 \\ \varphi_{D-\frac{1}{2}}^0 \end{pmatrix}$	1	0	2	$\begin{matrix} - \\ + \end{matrix}$
$\Psi = \begin{pmatrix} \psi_D \\ \psi \end{pmatrix}$	1	Q	2	$\begin{matrix} - \\ + \end{matrix}$
$V_{D\mu} = \begin{pmatrix} V_{D+\mu}^0 \\ V_{D0\mu}^0 \\ V_{D-\mu}^0 \end{pmatrix}$	1	0	3	$\begin{matrix} - \\ + \\ - \end{matrix}$

TABLE I. The quantum numbers of the new particles under the Electro-Weak (EW) and $SU(2)_D$ gauge groups.

The scalar potential for Φ_H and Φ_D reads:

$$V(\Phi_H, \Phi_D) = -\mu^2 \Phi_H^\dagger \Phi_H + \lambda(\Phi_H^\dagger \Phi_H)^2 - \mu_D^2 \Phi_D^\dagger \Phi_D + \lambda_D(\Phi_D^\dagger \Phi_D)^2 + \lambda_{\Phi_H \Phi_D} \Phi_H^\dagger \Phi_H \Phi_D^\dagger \Phi_D \quad (4)$$

This potential has non-trivial stationary points at

$$\begin{cases} v = \pm \sqrt{\frac{4\lambda_D \mu^2 - 2\lambda_{\Phi_H \Phi_D} \mu_D^2}{4\lambda\lambda_D - \lambda_{\Phi_H \Phi_D}^2}} \\ v_D = \pm \sqrt{\frac{4\lambda \mu_D^2 - 2\lambda_{\Phi_H \Phi_D} \mu^2}{4\lambda\lambda_D - \lambda_{\Phi_H \Phi_D}^2}} \end{cases}, \quad (5)$$

which define its minima if the following conditions are satisfied: $\mu \neq 0$, $\mu_D \neq 0$ and either $\{\lambda_{\Phi_H \Phi_D} < 0, \lambda > 0, \lambda_D > 0, \lambda_{\Phi_H \Phi_D}^2 < 4\lambda\lambda_D\}$ or $\{\lambda_{\Phi_H \Phi_D} > 0, 2\lambda\mu_D^2 > \lambda_{\Phi_H \Phi_D} \mu^2, 2\lambda_D \mu^2 > \lambda_{\Phi_H \Phi_D} \mu_D^2\}$.

The theory contains 6 massive gauge bosons (Z , W^\pm , V_{D0}^0 and $V_{D\pm}^0$) and therefore 6 Goldstone bosons correspond to their longitudinal components. The remaining 2 degrees of freedom correspond to physical scalars, which include the Higgs boson of the SM and another CP-even scalar. By denoting the neutral scalars in terms of their components in the unitary gauge as $\phi^0 = \frac{1}{\sqrt{2}}(v + h_1)$ and $\phi_{D-1/2}^0 = \frac{1}{\sqrt{2}}(v_D + \varphi_1)$, the mass terms of the scalar Lagrangian reads:

$$\mathcal{L}_m^S = (h_1 \ \varphi_1) \begin{pmatrix} \lambda v^2 & \frac{\lambda_{\Phi_H \Phi_D}}{2} v v_D \\ \frac{\lambda_{\Phi_H \Phi_D}}{2} v v_D & \lambda_D v_D^2 \end{pmatrix} \begin{pmatrix} h_1 \\ \varphi_1 \end{pmatrix}. \quad (6)$$

The mass eigenvalues can be obtained by diagonalising the mass matrix via a rotation matrix $V_S = \begin{pmatrix} \cos \theta_S & \sin \theta_S \\ -\sin \theta_S & \cos \theta_S \end{pmatrix}$ and read:

$$m_{h,H_D}^2 = \lambda v^2 + \lambda_D v_D^2 \mp \sqrt{(\lambda v^2 - \lambda_D v_D^2)^2 + \lambda_{\Phi_H \Phi_D}^2 v^2 v_D^2}, \quad (7)$$

with mixing angle $\sin \theta_S = \sqrt{2 \frac{m_{H_D}^2 v^2 \lambda - m_h^2 v_D^2 \lambda_D}{m_{H_D}^4 - m_h^4}}$.

The masses of the SM gauge bosons are not altered by the presence of Φ_D . The gauge bosons of $SU(2)_D$ are all degenerate in mass at tree level:

$$m_{V_D} \equiv m_{V_{D\pm}^0} = m_{V_{D0}^0} = \frac{g_D}{2} v_D. \quad (8)$$

This degeneracy is broken by the different fermionic loop corrections associated with the opposite \mathbb{Z}_2 parities of the $SU(2)_D$ gauge bosons. The only electrically neutral and massive \mathbb{Z}_2 -odd states of FPVDM scenarios are the $SU(2)_D$ gauge bosons $V_{D\pm}^0$ which are therefore the DM candidates.³

In the fermion sector, the component with $T_{3D} = 1/2$ gets only a VL mass, therefore

$$m_{\psi_D} = M_\Psi, \quad (9)$$

while the other fermion masses are generated after both scalars acquire a VEV. The fermionic mass matrix reads:

$$\mathcal{L}_m^f = (\bar{f}_L^{\text{SM}} \psi_L) \mathcal{M}_F \begin{pmatrix} f_R^{\text{SM}} \\ \psi_R \end{pmatrix}, \text{ with } \mathcal{M}_F = \begin{pmatrix} y \frac{v}{\sqrt{2}} & 0 \\ y' \frac{v_D}{\sqrt{2}} & M_\Psi \end{pmatrix}. \quad (10)$$

This mass matrix describes the mixing of a VL fermion with a SM fermion driven by Φ_D . The mass matrix can be diagonalised by two unitary matrices, $V_{L,R}$, leading to the mass eigenstates f and F , where f identifies the SM fermion and F its heavier partner:

$$\mathcal{L}_m^f = (\bar{f}_L F_L) \mathcal{M}_F^d \begin{pmatrix} f_R \\ F_R \end{pmatrix} = (\bar{f}_L F_L) V_{fL}^\dagger \mathcal{M}_F V_{fR} \begin{pmatrix} f_R \\ F_R \end{pmatrix}, \quad (11)$$

with $V_{fL,R} = \begin{pmatrix} \cos \theta_{fL,R} & \sin \theta_{fL,R} \\ -\sin \theta_{fL,R} & \cos \theta_{fL,R} \end{pmatrix}$. The mass eigenvalues are:

$$m_{f,F}^2 = \frac{1}{4} \left[y^2 v^2 + y'^2 v_D^2 + 2M_\Psi \mp \sqrt{(y^2 v^2 + y'^2 v_D^2 + 2M_\Psi)^2 - 8y^2 v^2 M_\Psi^2} \right]. \quad (12)$$

The fermion sector contains therefore a SM fermion with mass m_f , a \mathbb{Z}_2 -even partner with mass m_F and a \mathbb{Z}_2 -odd partner with mass m_{ψ_D} . The mass hierarchy is $m_f < m_{\psi_D} \leq m_F$.

The Yukawa parameters can be traded for the masses of the physical fermions as

$$y = \sqrt{2} \frac{m_f m_F}{m_{\psi_D} v}, \quad y' = \sqrt{2} \frac{\sqrt{(m_F^2 - m_{\psi_D}^2)(m_{\psi_D}^2 - m_f^2)}}{m_{\psi_D} v_D} \quad (13)$$

³ In principle, the introduction of VL neutrino partners could make the \mathbb{Z}_2 -odd member of the VL doublet a DM candidate, but a mixing in the neutrino sector would require further new physics to account for neutrino mass generation. This non-minimal scenario is not considered in the present analysis.

and the mixing angles as

$$\sin^2 \theta_{fL} = \frac{m_f^2}{m_{\psi_D}^2} \frac{m_F^2 - m_{\psi_D}^2}{m_F^2 - m_f^2}, \quad \sin^2 \theta_{fR} = \frac{m_F^2 - m_{\psi_D}^2}{m_F^2 - m_f^2}. \quad (14)$$

The left-handed mixing angle is suppressed by the $m_f^2/m_{\psi_D}^2$ ratio. The new fermion sector is completely decoupled in the limit $m_F = m_{\psi_D}$, for which $y = y_{\text{SM}} = \sqrt{2} \frac{m_f}{v}$, $y' = 0$, $\sin \theta_{fL} = \sin \theta_{fR} = 0$, so that the pure SM scenario is restored.

When the full flavour structure of the SM is taken into consideration, different possibilities can be considered. A VL fermion can interact with one or more SM flavours, plus there can be multiple VL fermions. The Cabibbo-Kobayashi-Maskawa (CKM) matrix of the SM might also receive contributions from new physics induced by the mixing of SM and VL quarks. In the following we assume that new VL fermions interact only with one SM flavour: in this case all the Lagrangian parameters can be traded for the masses of the physical states, the EW coupling constant g (or equivalently, the fine structure constant α_{EM}), the new gauge coupling g_D , the mixing angle between the scalar fields θ_S and the measured CKM parameters. Six independent input parameters are thus necessary to describe the new physics sector of the model, namely: g_D , M_{V_D} , m_{H_D} , $\sin \theta_S$, m_F , m_{ψ_D} . Notice that if there is no mixing in the scalar sector ($\theta_S = 0$), there is no Higgs portal at tree level.

Let us now discuss a specific realisation of the model, assuming only one VL partner interacting exclusively with the SM top quark and no mixing between h and H_D , i.e., $\theta_S = 0$. This choice significantly simplifies the Lagrangian: the Higgs sector of the SM is not affected by the new physics at tree-level and the potential of Φ_D has the very same structure as the Higgs potential. A mixing between h and H_D is induced only by fermionic loops and will be neglected in the following. The hierarchy between the masses in the fermion sector is $m_t < m_{t_D} \leq m_T$, while H_D can have any mass allowed by experimental bounds, including lighter than the SM Higgs boson. These choices are dictated, on the one hand, by minimality and, on the other hand, by a scenario where a non-abelian dark sector is connected to the SM exclusively through the fermion sector without a Higgs portal.

In our study we test this realisation of the model against multiple observables from cosmology, DM Direct and Indirect Detection (DD and ID) experiments and LHC searches. For this purpose the Lagrangian has been implemented in L^ANHEP [22] and FEYNRULES [23] while model files have been generated in CALCHEP [24], UFO [25] as well as FEYNARTS [26] formats and are available on the HEPMDB [27]. This implementation has been used in MICROMEGAS v5.2.7 [28] for the evaluation of various DM observables and for extracting the respective limits. The model implementation in UFO

format has been used in MG5_AMC [29] for the determination of the LHC constraints. Collider simulations have been performed at LO using the NNPDF3.0 LO set [30] through the LHAPDF6 library [31] (LHA index 262400). A simplified version of the model has been implemented to calculate cross-sections at one loop in MG5_AMC and FORMCALC9.8 [32].

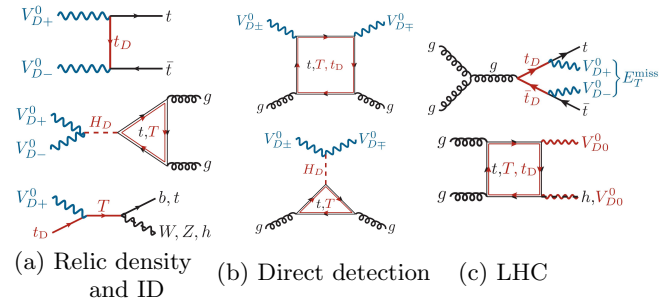


FIG. 1. (a) t -channel and resonant contributions to DM annihilation and DM-mediator co-annihilation processes. (b) Representative diagrams for DD processes. (c) Production processes at the LHC: $t\bar{t} + E_T^{\text{miss}}$, hV_{D0}^0 and $V_{D0}^0 V_{D0}^0$.

The measured amount of relic density is determined by the interplay of annihilation and co-annihilation processes shown in fig. 1(a). ID constraints are associated with DM annihilation rates at CMB time, excluding regions of parameter space where the injection into SM-plasma in the early Universe is too large to be consistent with CMB data. Both relic density and ID processes are tested against PLANCK data [33].

DD processes are represented by the diagrams in fig. 1(b) and tested against limits from XENON 1T [34].

The LHC bound has been obtained via testing of t_D pair production with subsequent decay into $V_{D\pm}^0$ and top quarks against CMS searches for top squark pair production decaying into DM. These analyses were done for the final states with opposite sign leptons and missing transverse energy E_T^{miss} [35], recast through the MADANALYSIS 5 framework [36, 37]. We also estimated the relevance of V_{D0}^0 pair production and associate production of V_{D0}^0 with the Higgs boson, occurring at LO via fermion loops. The tested processes are shown in fig. 1(c).

The complementarity of cosmological and collider constraints has been studied by performing a comprehensive scan over the parameter space (excluding the fixed parameter $\sin \theta_S = 0$) projected onto the $(g_D, m_{V_{D\pm}^0})$ plane, shown in fig. 2. The allowed parameter space is indicated by the green, cyan and blue regions, presenting generic DM annihilation, dominated by the t -channel diagram of fig. 1(a), resonance (H_D) and DM- t_D co-annihilation regions, respectively, which satisfy the relic density constraint from PLANCK within 5%. The generic DM annihilation determines a lower limit on g_D as a function of $m_{V_{D\pm}^0}$. At the same time the H_D resonant region allows to reduce g_D values by up to two orders

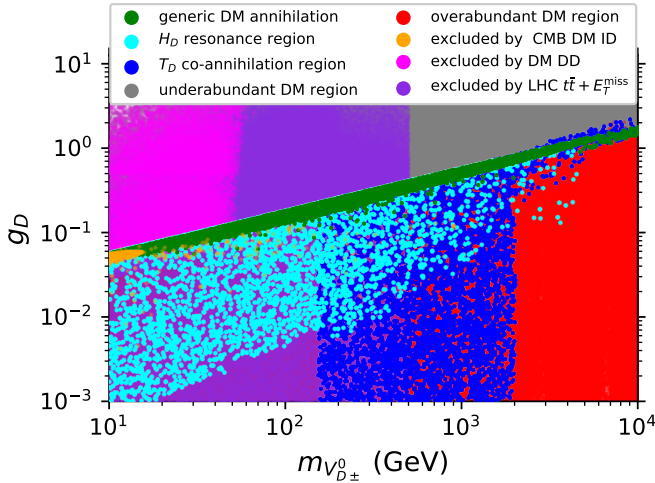


FIG. 2. Excluded and allowed region of the parameter space of the model from the full five-dimensional scan ($\sin \theta_S = 0$) of the parameter space projected into a $(g_D, m_{V_{D\pm}^0})$ plane.

of magnitude, while the strong DM- t_D co-annihilation channel allows for even lower values of g_D for not so heavy DM. For $m_{V_{D\pm}^0}$ above 2 TeV, however, both the co-annihilation and resonant DM annihilation mechanisms are not effective anymore. Therefore, the region with low g_D and large $m_{V_{D\pm}^0}$ has an over-abundant relic density, as indicated by the red colour. Notice also that the regions with low $m_{V_{D\pm}^0}$ and large g_D values are partly excluded by DD and/or ID experiments as indicated by magenta and orange points, respectively. The region of DM masses which can be tested and excluded by the LHC is $m_{V_{D\pm}^0} \lesssim 400$ GeV, represented by the violet region.

To assess the relative role of the different constraints we identify representative benchmarks, characterised by different gauge couplings, $g_D = 0.05$ and $g_D = 0.5$, and fixed values for the masses, $m_T = 1600$ GeV and $m_{H_D} = 1000$ GeV. For these points the gauge coupling is small enough to allow a perturbative treatment in a region of parameter space which can be tested by both collider and cosmological observables and the \mathbb{Z}_2 -even partner of the top and new scalar H_D are heavy enough to easily evade current LHC bounds based on their decays into SM final states. We show in fig. 3 the exclusion regions in the $\{m_{t_D}, m_{V_{D\pm}^0}\}$ and $\{m_{t_D}, 1 - m_{V_{D\pm}^0}/m_{t_D}\}$ planes to highlight the low $m_{V_{D\pm}^0}$ or low $m_{t_D} - m_{V_{D\pm}^0}$ regions, respectively. The masses of the DM candidate $V_{D\pm}^0$ and mediator t_D are left as free parameters.

The measured amount of relic density is satisfied only in specific regions: for $g_D = 0.05$ most of the parameter space predicts an over-abundant relic density, except for an area where the mass difference between t_D and the DM is less than $\sim 10\%$ of the mediator mass (where t_D - t_D and DM- t_D co-annihilation processes dominate), a small area around $m_{V_{D\pm}^0} = m_{H_D}/2$ (DM annihilation via

resonant H_D) and for $m_{V_{D\pm}^0} \lesssim 10$ GeV. For larger values of g_D , annihilation processes become more effective, reducing the size of the excluded area in the lower $m_{V_{D\pm}^0}$ region, and eventually extending the under-abundant relic density region. The radiative mass split of the V_{D0}^0 and $V_{D\pm}^0$ bosons, $\Delta m_V = m_{V_{D\pm}^0} - m_{V_{D0}^0}$, due to fermion-loop mass corrections, plays a special role in the determination of relic density and ID rates. The leading contribution to Δm_V is determined by T and t_D loops to be

$$\Delta m_V = \frac{\epsilon^2 g_D^2 m_T^2}{32\pi^2 m_{V_{D\pm}^0}} + o(\epsilon^2), \quad \text{where } \epsilon = \frac{m_T^2 - m_{t_D}^2}{m_T^2}. \quad (15)$$

Since $\Delta m_V > 0$, the enhancement of the $V_{D+}^0 V_{D-}^0 \rightarrow V_{D0}^0 V_{D0}^0$ process affects the relic density and ID signals. The complementarity of various constraints is especially evident for small values of g_D in the low $m_{V_{D\pm}^0}$ region. The region excluded by ID corresponds to small values of $m_{V_{D\pm}^0}$ for $g_D = 0.05$, largely overlapping with the region excluded by relic density, and rapidly vanishes as g_D increases. The excluded DD regions correspond to the limiting values $m_{t_D} \rightarrow m_t$ and $m_{t_D} \rightarrow m_T$ for low values of $m_{V_{D\pm}^0}$. In these regions the contribution of triangle loops becomes negligible with respect to the enhanced box diagrams (see fig. 1(b)), which otherwise interfere destructively, reducing the cross-section of the DD process and evading the constraints. The LHC bound is almost independent of the mass of t_D until its mass difference with the DM reaches the top-quark threshold: in that region the E_T^{miss} decreases and the sensitivity of the CMS search reduces, allowing a small mass-gap region. As the process is QCD initiated, the bound is almost independent on other parameters of the model. Processes of V_{D0}^0 pair production and associate production of V_{D0}^0 with the Higgs boson have cross-sections which scale with g_D^4 and g_D^2 respectively and are testable ($\sigma \gtrsim \mathcal{O}(10 \text{ fb})$) only for small ($\lesssim 100$ GeV) values of $m_{V_{D\pm}^0}$ which partly excluded by ID constraints. The model has an important feature, especially for small values of g_D in the small DM- t_D mass-gap region where the correct relic density is reproduced. In this region t_D is long-lived (its lifetime in the small mass-gap region is shown in fig. 3) and can be probed by dedicated searches at the LHC or future colliders. Different T or H_D masses would not modify this qualitative picture.

This minimal realisation of FPVDM has already great potential to explain DM phenomena together with several important implications for collider and non-collider DM searches. Non-minimal FPVDM realisations would imply even richer sets of predictions and can be used to explain outstanding observed anomalies. For example, if the VL fermion interacts with the leptonic sector of the SM, new contributions might explain current lepton flavour anomalies [38] or $(g-2)_\mu$ [39] and at the same time would provide novel physics cases for future e^+e^-

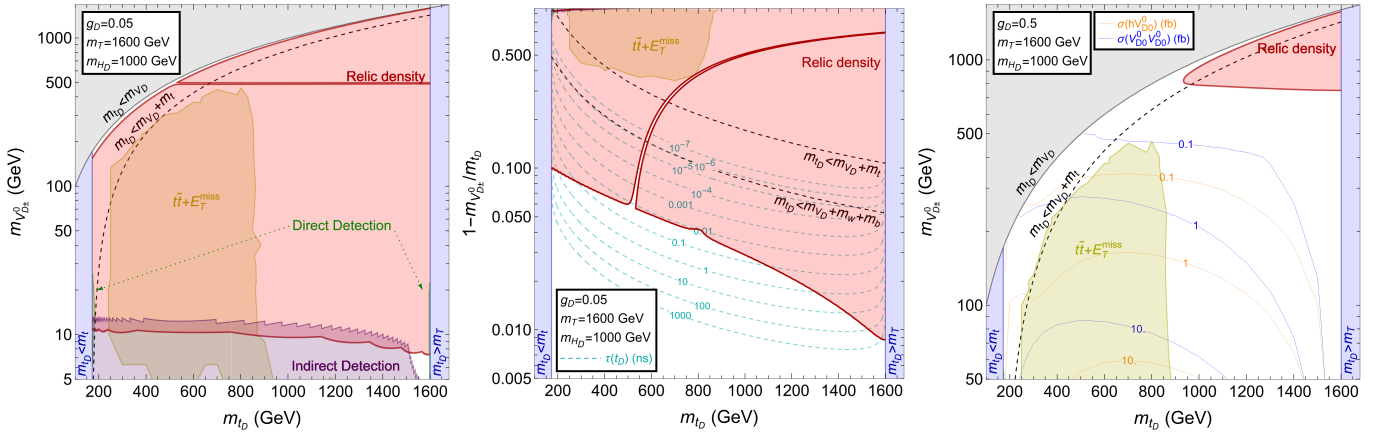


FIG. 3. Combination of constraints from LHC, relic density, DD and ID for the benchmark points in the $\{m_{t_D}, m_{V_{D\pm}^0}\}$ (left and right panels) and $\{m_{t_D}, 1 - m_{V_{D\pm}^0}/m_{t_D}\}$ (center panel) planes. The coloured regions are excluded. For relic density, the under-abundant region is considered as allowed and the borders of the excluded region correspond to the measured relic density value. Contours corresponding to different t_D lifetimes are shown for the small mass splitting region.

colliders [40–43]. Including mixing in the scalar sector, further VL partners or additional interactions of the same VL representation would open up a vast range of possibilities for future studies, both phenomenological and experimental, and would allow one to explore the complementarity between collider and non-collider observables in multiple scenarios.

ACKNOWLEDGEMENTS

AB and SM acknowledge support from the STFC Consolidated Grant ST/L000296/1 and are partially financed through the NExT Institute. LP’s work is supported by the Knut and Alice Wallenberg foundation under the SHIFT project, grant KAW 2017.0100. AD is grateful to the LABEX Lyon Institute of Origins (ANR-10-LABX-0066) for its financial support within the program “Investissements d’Avenir”. NT is supported by the scholarship from the Development and Promotion of Science and Technology Talents Project (DPST). All authors acknowledge the use of the IRIDIS High-Performance Computing Facility and associated support services at the University of Southampton in completing this work.

* a.belyaev@soton.ac.uk

† deandrea@ipnl.in2p3.fr

‡ s.moretti@soton.ac.uk; stefano.moretti@physics.uu.se

§ luca.panizzi@physics.uu.se

¶ nakorn.thongyoi@gmail.com

[1] T. Hambye, Hidden vector dark matter, JHEP **01**, 028, arXiv:0811.0172 [hep-ph].

- [2] F. Chen, J. M. Cline, and A. R. Frey, Nonabelian dark matter: Models and constraints, Phys. Rev. D **80**, 083516 (2009), arXiv:0907.4746 [hep-ph].
- [3] J. Diaz-Cruz and E. Ma, Neutral SU(2) Gauge Extension of the Standard Model and a Vector-Boson Dark-Matter Candidate, Phys. Lett. B **695**, 264 (2011), arXiv:1007.2631 [hep-ph].
- [4] S. Bhattacharya, J. Diaz-Cruz, E. Ma, and D. Wegman, Dark Vector-Gauge-Boson Model, Phys. Rev. D **85**, 055008 (2012), arXiv:1107.2093 [hep-ph].
- [5] E. Koorambas, Vector Gauge Boson Dark Matter for the SU(N) Gauge Group Model, Int. J. Theor. Phys. **52**, 4374 (2013).
- [6] S. Fraser, E. Ma, and M. Zakeri, SU(2)_N model of vector dark matter with a leptonic connection, Int. J. Mod. Phys. A **30**, 1550018 (2015), arXiv:1409.1162 [hep-ph].
- [7] J. Hubisz and P. Meade, Phenomenology of the lightest Higgs with T-parity, Phys. Rev. D **71**, 035016 (2005), arXiv:hep-ph/0411264.
- [8] W.-C. Huang, Y.-L. S. Tsai, and T.-C. Yuan, G2HDM : Gauged Two Higgs Doublet Model, JHEP **04**, 019, arXiv:1512.00229 [hep-ph].
- [9] P. Ko and Y. Tang, Residual Non-Abelian Dark Matter and Dark Radiation, Phys. Lett. B **768**, 12 (2017), arXiv:1609.02307 [hep-ph].
- [10] B. Barman, S. Bhattacharya, S. K. Patra, and J. Chakraborty, Non-Abelian Vector Boson Dark Matter, its Unified Route and signatures at the LHC, JCAP **12**, 021, arXiv:1704.04945 [hep-ph].
- [11] W.-C. Huang, H. Ishida, C.-T. Lu, Y.-L. S. Tsai, and T.-C. Yuan, Signals of New Gauge Bosons in Gauged Two Higgs Doublet Model, Eur. Phys. J. C **78**, 613 (2018), arXiv:1708.02355 [hep-ph].
- [12] B. Barman, S. Bhattacharya, and M. Zakeri, Multipartite Dark Matter in SU(2)_N extension of Standard Model and signatures at the LHC, JCAP **09**, 023, arXiv:1806.01129 [hep-ph].
- [13] B. Barman, S. Bhattacharya, and M. Zakeri, Non-Abelian Vector Boson as FIMP Dark Matter, JCAP **02**, 029, arXiv:1905.07236 [hep-ph].

- [14] T. Abe, M. Fujiwara, J. Hisano, and K. Matsushita, A model of electroweakly interacting non-abelian vector dark matter, *JHEP* **07**, 136, arXiv:2004.00884 [hep-ph].
- [15] T. A. Chowdhury and S. Saad, Non-Abelian vector dark matter and lepton g-2, *JCAP* **10**, 014, arXiv:2107.11863 [hep-ph].
- [16] N. Baouche, A. Ahriche, G. Faisel, and S. Nasri, Phenomenology of the hidden SU(2) vector dark matter model, *Phys. Rev. D* **104**, 075022 (2021), arXiv:2105.14387 [hep-ph].
- [17] J. B. Jiménez, D. Bettoni, and P. Brax, Charged dark matter and the H_0 tension, *Phys. Rev. D* **103**, 103505 (2021), arXiv:2004.13677 [astro-ph.CO].
- [18] T. Ma and G. Cacciapaglia, Fundamental Composite 2HDM: SU(N) with 4 flavours, *JHEP* **03**, 211, arXiv:1508.07014 [hep-ph].
- [19] Y. Wu, T. Ma, B. Zhang, and G. Cacciapaglia, Composite Dark Matter and Higgs, *JHEP* **11**, 058, arXiv:1703.06903 [hep-ph].
- [20] S. Baek, P. Ko, and P. Wu, Heavy quark-philic scalar dark matter with a vector-like fermion portal, *JCAP* **07**, 008, arXiv:1709.00697 [hep-ph].
- [21] S. Colucci, B. Fuks, F. Giacchino, L. Lopez Honorez, M. H. G. Tytgat, and J. Vandecasteele, Top-philic Vector-Like Portal to Scalar Dark Matter, *Phys. Rev. D* **98**, 035002 (2018), arXiv:1804.05068 [hep-ph].
- [22] A. Semenov, Lanhep—a package for the automatic generation of feynman rules in field theory. version 3.0, *Computer Physics Communications* **180**, 431–454 (2009).
- [23] A. Alloul, N. D. Christensen, C. Degrande, C. Duhr, and B. Fuks, FeynRules 2.0 - A complete toolbox for tree-level phenomenology, *Comput. Phys. Commun.* **185**, 2250 (2014), arXiv:1310.1921 [hep-ph].
- [24] A. Belyaev, N. D. Christensen, and A. Pukhov, CalcHEP 3.4 for collider physics within and beyond the Standard Model, *Comput. Phys. Commun.* **184**, 1729 (2013), arXiv:1207.6082 [hep-ph].
- [25] C. Degrande, C. Duhr, B. Fuks, D. Grellscheid, O. Mattelaer, and T. Reiter, UFO - The Universal FeynRules Output, *Comput. Phys. Commun.* **183**, 1201 (2012), arXiv:1108.2040 [hep-ph].
- [26] T. Hahn, Generating Feynman diagrams and amplitudes with FeynArts 3, *Comput. Phys. Commun.* **140**, 418 (2001), arXiv:hep-ph/0012260.
- [27] M. Bondarenko, A. Belyaev, J. Blandford, L. Basso, E. Boos, V. Bunichev, *et al.*, High Energy Physics Model Database : Towards decoding of the underlying theory (within Les Houches 2011: Physics at TeV Colliders New Physics Working Group Report), (2012), arXiv:1203.1488 [hep-ph].
- [28] G. Belanger, A. Mjallal, and A. Pukhov, Recasting direct detection limits within micrOMEGAs and implication for non-standard Dark Matter scenarios, *Eur. Phys. J. C* **81**, 239 (2021), arXiv:2003.08621 [hep-ph].
- [29] J. Alwall, R. Frederix, S. Frixione, V. Hirschi, F. Maltoni, O. Mattelaer, H. S. Shao, T. Stelzer, P. Torrielli, and M. Zaro, The automated computation of tree-level and next-to-leading order differential cross sections, and their matching to parton shower simulations, *JHEP* **07**, 079, arXiv:1405.0301 [hep-ph].
- [30] R. D. Ball *et al.* (NNPDF), Parton distributions for the LHC Run II, *JHEP* **04**, 040, arXiv:1410.8849 [hep-ph].
- [31] A. Buckley, J. Ferrando, S. Lloyd, K. Nordström, B. Page, M. Rüfenacht, M. Schönherr, and G. Watt, LHAPDF6: parton density access in the LHC precision era, *Eur. Phys. J. C* **75**, 132 (2015), arXiv:1412.7420 [hep-ph].
- [32] T. Hahn, S. Paßehr, and C. Schappacher, FormCalc 9 and Extensions, *PoS* **LL2016**, 068 (2016), arXiv:1604.04611 [hep-ph].
- [33] N. Aghanim *et al.* (Planck), Planck 2018 results. VI. Cosmological parameters, *Astron. Astrophys.* **641**, A6 (2020), [Erratum: *Astron. Astrophys.* 652, C4 (2021)], arXiv:1807.06209 [astro-ph.CO].
- [34] E. Aprile *et al.* (XENON), Dark Matter Search Results from a One Ton-Year Exposure of XENON1T, *Phys. Rev. Lett.* **121**, 111302 (2018), arXiv:1805.12562 [astro-ph.CO].
- [35] A. M. Sirunyan *et al.* (CMS), Search for top squarks and dark matter particles in opposite-charge dilepton final states at $\sqrt{s} = 13$ TeV, *Phys. Rev. D* **97**, 032009 (2018), arXiv:1711.00752 [hep-ex].
- [36] E. Conte and B. Fuks, Confronting new physics theories to LHC data with MADANALYSIS 5, *Int. J. Mod. Phys. A* **33**, 1830027 (2018), arXiv:1808.00480 [hep-ph].
- [37] S. Bein, S.-M. Choi, B. Fuks, S. Jeong, D. W. Kang, J. Li, and J. Sonneveld, Implementation of a search for stops in the di-lepton + missing energy channel (35.9 fb⁻¹; 13 TeV; CMS-SUS-17-001) (2021).
- [38] A. Crivellin and M. Hoferichter, Hints of lepton flavor universality violations, *Science* **374**, 1051 (2021), arXiv:2111.12739 [hep-ph].
- [39] B. Abi *et al.* (Muon g-2), Measurement of the Positive Muon Anomalous Magnetic Moment to 0.46 ppm, *Phys. Rev. Lett.* **126**, 141801 (2021), arXiv:2104.03281 [hep-ex].
- [40] A Multi-TeV Linear Collider Based on CLIC Technology: CLIC Conceptual Design Report 10.5170/CERN-2012-007 (2012).
- [41] The International Linear Collider Technical Design Report - Volume 2: Physics, (2013), arXiv:1306.6352 [hep-ph].
- [42] F. An *et al.*, Precision Higgs physics at the CEPC, *Chin. Phys. C* **43**, 043002 (2019), arXiv:1810.09037 [hep-ex].
- [43] A. Abada *et al.* (FCC), FCC-ee: The Lepton Collider: Future Circular Collider Conceptual Design Report Volume 2, *Eur. Phys. J. ST* **228**, 261 (2019).